

Effects of mono-substituting chelating agents on BaTiO₃ prepared by the sol–gel process

WOEI-KWO KUO, YONG-CHIEN LING

Department of Chemistry, National Tsing Hua University, Hsinchu 30043 Taiwan

BaTiO₃ of various grain size was prepared by the sol–gel process from Ti(OR)₄ (R = isoC₃H₇ or C₄H₉) + Ba(CH₃COO)₂ + chelating agent CH₃COCH₂COR' (R' = CH₃ or OC₂H₅) in a composition of equal molar ratio. Fourier transform infrared and fast atom bombardment mass spectrometry analyses suggested that the chelating agent substituted for one of the OR groups in Ti(OR)₄ to form Ti(OR)₃(CH₃COCHCOR'). The gelation time varied from 3 to 5 months and diminished with increasing steric hindrance. The amorphous gel was crystallized into cubic phase BaTiO₃ upon heating above 650 °C. The tetragonal phase was obtained after heating for 1 h at 1350 °C with the theoretical Ba/Ti ratio and 1.0096 *c/a* value. The measured dielectric constants diminished with increasing grain size. The results illustrated the merits of altering the chemistry of the precursors to control the properties of the BaTiO₃.

1. Introduction

BaTiO₃-based materials have found wide applications in the electrical and electronic industries because of their high dielectric constants, ferroelectric property, and positive temperature coefficient of electrical resistivity (PTCR). Various studies have been performed with the aim of establishing the correlations between the preparation route and their microstructure, which in turn affect their functional properties.

Additions of oxides such as CaO, ZrO₂ and CaTiO₃ [1–3] during the preparation of BaTiO₃ by solid-state reactions have been used to study their defect chemistry and dielectric property, and to control the grain size and grain boundary characteristics [4–6] for understanding the relation between microstructure and dielectric properties. Similar studies based on solid-state reactions have focused on PTCR-related phenomena [7–9]. Rigorous quality control of the starting raw materials is crucial to the reliability and reproducibility of BaTiO₃ prepared by solid-state reactions. To alleviate these difficulties, the sol–gel method has gained increasing attention [10, 11] because it can yield homogeneous, high purity and fine ceramic powder with excellent stoichiometry. In the sol–gel method, problems from hydrolysis and condensation of metal alkoxide M(OR)₄ reactants are usually encountered. The formation of M–O–M products degrades the stability of the precursors and fails to yield the final ceramic products. The hydrolysis problem has been investigated by the addition of glacial acetic acid and acetylacetone to the Ti(OR)₄. This study was limited to the Ti(OR)₄ reactants rather than the products, however [12].

The present study describes a modified sol–gel process to prepare BaTiO₃ using mono-substituting agents to alter the precursors formed in the normal sol–gel process [10]. The aim is to provide a gel with a

longer gelation time which would be more feasible for different processing schemes. The results of using Ti(OR)₄ (R = isoC₃H₇ or C₄H₉) + Ba(CH₃COO)₂ + chelating agent CH₃COCH₂COR' (R' = CH₃ or OC₂H₅) are reported. The preparation of the gel precursors, their appearance, composition, thermal analyses, and the crystal phase and microstructural characterization of both intermediate products and the final BaTiO₃ powders are described. The properties of the gels and powders prepared by the modified sol–gel process are compared with those prepared by the existing Ti(O-isoC₃H₇)₄ + Ba(CH₃COO)₂ process. The sequence of preparation reactions is investigated to explain the changes in microstructure and functional properties.

2. Experimental procedure

2.1. Preparation of BaTiO₃ precursors

All starting materials were reagent-grade chemicals. In the following, Ba(CH₃COO)₂, Ti(O-isoC₃H₇)₄, Ti(O-C₄H₉)₄, CH₃COCH₂COCH₃ and CH₃COCH₂COOC₂H₅ will be denoted as Ba(Ac)₂, Ti(O-iPr)₄, Ti(O-Bu)₄, AcAc and EtAc, respectively. BaTiO₃ precursors were prepared by two different methods. In the first method, 0.025 mol Ba(Ac)₂ was added to 25 ml propionic acid. The mixture was heated to 80 °C to yield a transparent solution. Then, 0.025 mol Ti(O-iPr)₄ or Ti(O-Bu)₄, was added slowly to this solution with a syringe to yield a yellow muddy solution. After being slowly heated to 110 °C, 0.025 mol of AcAc or EtAc was added. The combined solutions were continuously stirred for 3 h to yield the BaTiO₃ precursor. This method will be called Ti–Ba–Ac.

To confirm the substitution of the chelating agent for a single OR group in Ti(OR)₄, the BaTiO₃ pre-

cursor was prepared by a second method. $\text{Ti}(\text{OR})_4$ was allowed to react directly with the chelating agent in a nitrogen atmosphere at room temperature. $\text{Ba}(\text{Ac})_2$ solution dissolved in propionic acid was then added dropwise at 80°C . The combined solutions were slowly heated to 110°C to allow the reaction to occur. This method will be called Ti–Ac–Ba. Both reactions were performed under a dry N_2 atmosphere and reflux conditions. The traditional method not using any chelating agent will be denoted as the Ti–Ba method.

2.2. Thermal treatments and analyses

The BaTiO_3 precursor prepared by the Ti–Ac–Ba method was analysed by Fourier transform infrared spectroscopy (FT-IR) to confirm the substitution of chelating agent for a single OR group. Subsequent thermal treatments and analyses were performed on BaTiO_3 precursor prepared by the Ti–Ba–Ac method. FT-IR analyses were carried out first to identify the structure of the BaTiO_3 precursor. The proposed structure was further confirmed using fast atom bombardment mass spectrometry (FAB-MS). Thermogravimetric analysis/differential scanning calorimetry (TGA/DSC) were carried out under a dry O_2/N_2 atmosphere to monitor the decomposition and transformation temperature of the gels, previously dried at 180°C for 3 h. In order to convert the BaTiO_3 gels into ceramic, the gels were calcined for 1 h at 650 and 800°C to form white powders. The powders from 800°C were dry-pressed into pellets which were subsequently sintered for 1 h at 1350°C to yield bulk BaTiO_3 samples. All calcining and sintering processes were carried out in an electric furnace with an air atmosphere. The powder X-ray diffraction (XRD) technique was used to identify the crystal structure. Scanning electron microscopy (SEM) was used for microstructural characterization. The Ba/Ti ratio was measured using inductively-coupled plasma atomic emission spectroscopy (ICP-AES). Electrical measurement was done using a computerized impedance vectorial analyser.

3. Results and discussion

3.1. Chemical and physical properties of precursors

The composition, appearance and gelation time of precursors prepared by the Ti–Ba–Ac method are shown in Table I. The $\text{Ti}(\text{O}-i\text{Pr})_4 + \text{EtAc}$ system was not included in this study. In this system, transparent crystalline precursors inhibited the subsequent gel formation. Similar observations were reported before [13]. The gelation time varied with composition. Precursor I did not convert into gel even after 5 months. Precursors II and III became gels after 3 months. This difference was ascribed to the stronger steric effect between the ligands in precursor II (and III) than that in precursor I as Fig. 1 depicts. Both the size of the $(\text{O}-\text{Bu})$ group in $\text{Ti}(\text{O}-\text{Bu})_4$ and the (OC_2H_5) group in EtAc are larger than that of the $(\text{O}-i\text{Pr})$ group in $\text{Ti}(\text{O}-i\text{Pr})_4$ and the (CH_3) group in AcAc, respectively.

TABLE I Composition, appearance and gelation time of precursors

Precursor	Composition	Appearance	Gelation time (months)
I	$\text{Ti}(\text{O}-i\text{Pr})_4 + \text{AcAc}$	Dark red	> 5
II	$\text{Ti}(\text{O}-\text{Bu})_4 + \text{AcAc}$	Dark red	3
III	$\text{Ti}(\text{O}-\text{Bu})_4 + \text{EtAc}$	Light yellow	3

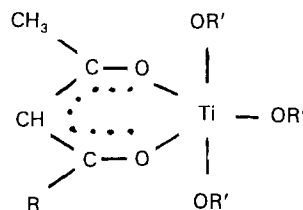


Figure 1 Structure of the mono-substituted products from $\text{Ti}(\text{OR})_4$ and chelating agent AcAc. For precursor I, $\text{R} = \text{CH}_3$ and $\text{R}' = \text{isoC}_3\text{H}_7$; for precursor II, $\text{R} = \text{CH}_3$ and $\text{R}' = \text{C}_4\text{H}_9$; for precursor III, $\text{R} = \text{OC}_2\text{H}_5$ and $\text{R}' = \text{C}_4\text{H}_9$.

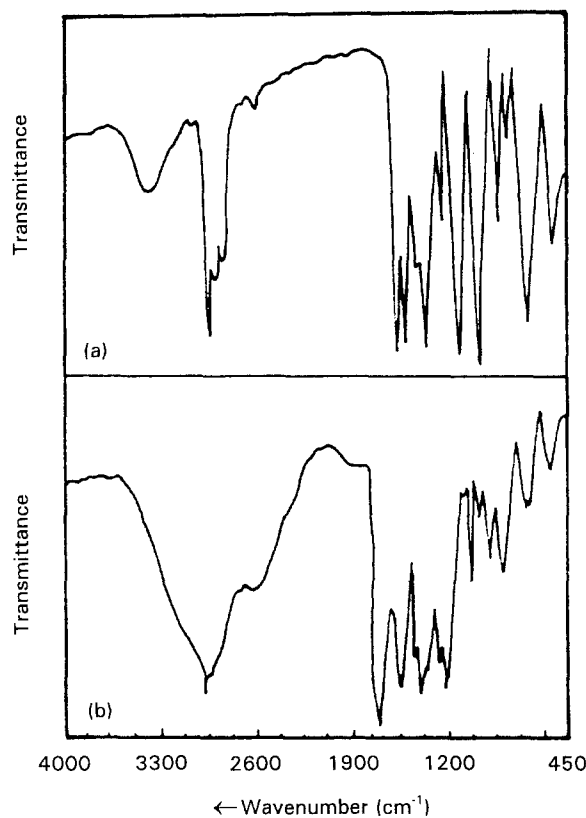


Figure 2 Infrared spectra of (a) intermediate products of $\text{Ti}(\text{O}-i\text{Pr})_4$ reacting with AcAc, and (b) final products after adding $\text{Ba}(\text{Ac})_2$ and propionic acid to (a).

Accordingly, the increasing steric effect between these larger ligands would degrade the stability of precursors in the sequence $\text{III} > \text{II} > \text{I}$ (most stable) when the coordination number of Ti changes from 4 to 5. The degradation in stability causes $\text{Ti}(\text{OR})_4$ to become a corner-sharing $-\text{Ti}-\text{O}-\text{Ti}-$ polymer more easily. The corresponding gelation time is thus shorter. Nevertheless, the gelation time of all three

precursors is much longer than the time of several days obtained by the traditional Ti–Ba method. These results coincide with the increased gelation time gained by adding chelating agents to the PbTiO_3 system [14].

The infrared spectrum (Fig. 2a) of the intermediate products of $\text{Ti}(\text{O}-i\text{Pr})_4$ reacting with AcAc by the Ti–Ac–Ba method has characteristic peaks at 1593 and 1378 cm^{-1} which are assigned to the asymmetric and symmetric C–O–Ti stretching vibrations, respectively. The –C–O– group comes from the AcAc. The peak around 1524 cm^{-1} is assigned to $\text{C}=\text{C}=\text{C}$ resonance. The broad band at 3395 cm^{-1} is assigned to *i*-PrOH formed by the substitution of an O–iPr group in $\text{Ti}(\text{O}-i\text{Pr})_4$ by AcAc. These absorption peaks confirm the existence of a substitution reaction with the chelating reagent. Fig. 2b shows the infrared spectrum of the final products of the Ti–Ac–Ba method. The peak at 1714 cm^{-1} is assigned to the –CO– group of the reaction by-product isopropyl acetate. This peak is usually overlapped by the –CO– group from propionic acid. The peaks at 1560 and 1406 cm^{-1} are assigned to the asymmetric and symmetric $-\text{COO}^-$ stretching vibrations in $\text{Ba}(\text{Ac})_2$, respectively. It is noted that these peaks are overlapped

by the $\text{C}=\text{C}=\text{C}$ resonance peak from Fig. 2a.

Fig. 3 shows the infrared spectra of precursors I, II, and III from the Ti–Ac–Ba method. The major differences between these spectra are in the wavenumber range 1400 to 1600 cm^{-1} because of the asymmetric and symmetric stretching vibrations of $-\text{COO}^-$ ($\nu_s(\text{COO})$ and $\nu_{as}(\text{COO})$). The frequency separation ($\Delta\nu$) between these two peaks strongly depends on the bonding modes of the acetate ($-\text{COO}^-$) group [15]. The results are detailed in Table II. The $\Delta\nu$ values are between 140 and 160 cm^{-1} and can be assigned to bridging and ionic acetate groups. Precursor I with a $\Delta\nu$ value of 154 cm^{-1} is more likely to exist in bridging bonding form. Precursors II and III with $\Delta\nu$ values of 146 and 141 cm^{-1} , respectively, are more likely to exist in ionic bonding form. The similarity between the infrared spectrum of Fig. 2(b) and the three spectra in

TABLE II Asymmetric and symmetric stretching vibrations of $-\text{COO}^-$ and the corresponding frequency separation

Precursor	$\nu_{as}(\text{COO})$ (cm^{-1})	$\nu_s(\text{COO})$ (cm^{-1})	$\Delta\nu$ (cm^{-1})
I	1561	1407	154
II	1563	1417	146
III	1559	1418	141

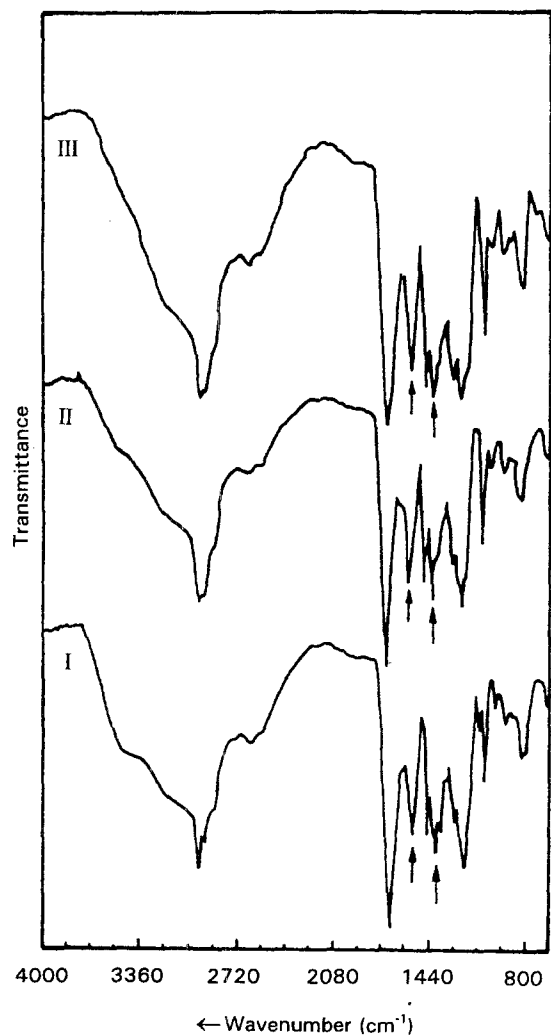


Figure 3 Infrared spectra of precursors I, II, and III obtained after using the Ti–Ba–Ac method. The arrows denote the $\nu_s(\text{COO})$ and $\nu_{as}(\text{COO})$ absorption peaks.

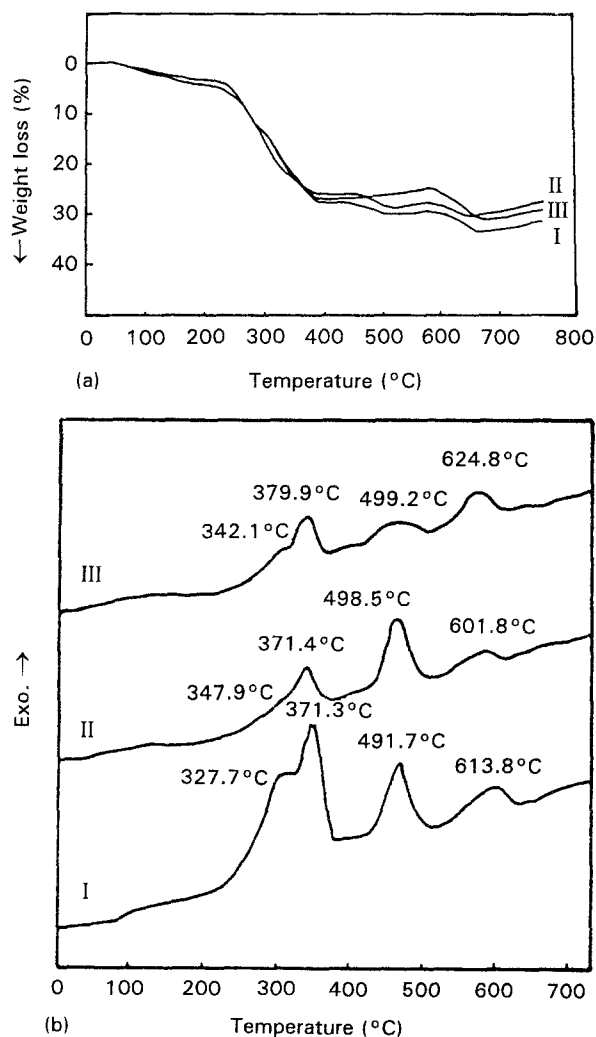


Figure 4 (a) TGA and (b) DSC curves of the thermal degradation of precursors I, II and III.

Fig. 3 suggests the existence of a mono-substituting reaction in the sol-gel system.

FAB-MS analyses of precursors I and II yield similar dominant peaks at m/z values of 196, 210, 303, 494 and 512. They were assigned as $[\text{Ba}(\text{CH}_3\text{COO})]^+$, $[(\text{BaO})(\text{CHCOO})]^+$, $[\text{Ti}(\text{AcAc})(\text{BaO}) + 3\text{H}]^+$, $[\text{I} + 3\text{H}]^+$ or $[\text{II} - \text{CH}_2 + 3\text{H}]^+$, and $[\text{I}(\text{H}_2\text{O}) + 3\text{H}]^+$ or $[\text{II}(\text{H}_2\text{O}) - \text{CH}_2 + 3\text{H}]^+$, respectively. The formation of protonated and hydrated molecular ions with m/z values of 494 and 512 confirms the existence of mono-substituting reactions in the sol-gel system.

3.2. Thermal analyses

The TGA and DSC curves of the thermal degradation of precursors I, II and III are shown in Fig. 4. There is no significant loss of weight below 250 °C (Fig. 4a) because the propionic acid solvent in the sample was almost vapourized in advance by the thermal treatment. A similar conclusion can be drawn from the DSC results (Fig. 4b) since no distinct changes are observed in the temperature range below 250 °C. Three distinct steps of weight loss are observed in the TGA curves. The first is around 250–400 °C with about 26–27% weight loss. Two large exothermic peaks appear in the corresponding DSC curves. Therefore, this step is due to the liberation of residual propionic acid and ester products, and their successive combustion. The second is around 400–500 °C with about 2% weight loss for precursors I and II and almost null for precursor III. In the DSC curves, a similar conclusion can be drawn as the intensity of the exothermic peak for precursors I and II is more intense than that of precursor III. This step is due to the pyrolysis of Ti-bound chelating agents. Precursors I and II are more stable than precursor III and accordingly liberate more material at higher temperature. The third step is around 550–650 °C accompanied by a broad exothermic peak. According to the XRD results, crystallization of BaTiO_3 began at 650 °C. Moreover, the weight loss is minimal and the weight stays unchanged afterwards. From these results, the third step corresponds to the conversion of gel into ceramic.

3.3. Crystal phase characterization

XRD analyses reveal that the dried gel starts to have a crystalline structure after thermal treatment at 650 °C for 1 h. The X-ray diffraction patterns of precursors I, II and III sintered at various temperature are shown in Fig. 5. At 650 °C (Fig. 5a) the crystal phase of the precipitated BaTiO_3 is cubic. This observation accords with the results obtained from TGA/DSC analyses. This temperature is about 50 °C higher than the crystallization temperature from the traditional Ti-Ba method. This difference is possibly due to the chemical structure of the precursor being more bulky and the Ti-chelating agent bond stronger when using this modified sol-gel method. At 800 °C (Fig. 5b) the crystal phase is still cubic. At 1350 °C (Fig. 5c) the 002 line is split into 002 and 200 lines. This observation

clearly suggests that the crystal phase of BaTiO_3 transforms from cubic form into tetragonal form [16]. The tetragonality (lattice constant ratio c/a) calculated using the peak intensity from 002 and 200 lines [17] is about 1.0096.

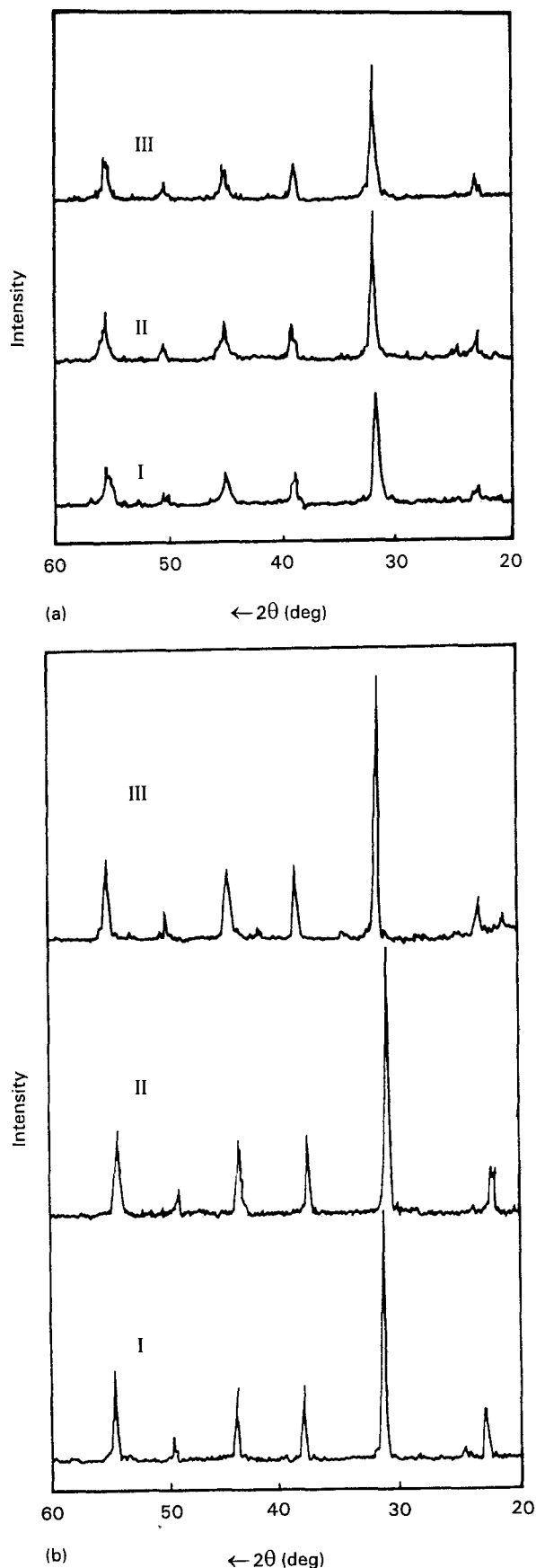


Figure 5 XRD patterns of precursors I, II and III as a function of sintering conditions. (a) 1 h at 650 °C, (b) 1 h at 800 °C, (c) 1 h at 1350 °C.

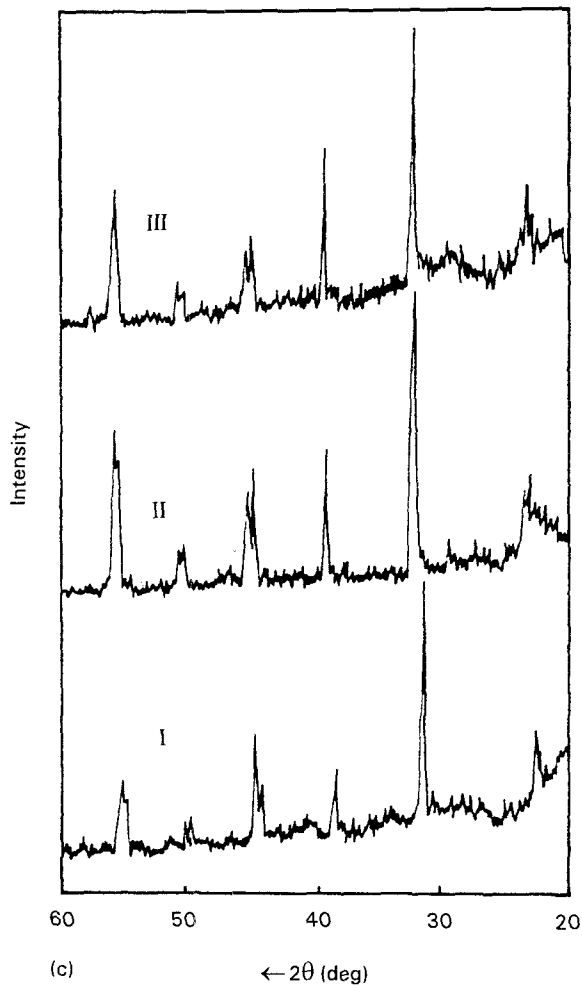


Figure 5 (Continued)

3.4. Microstructural characterization

The microstructures of powders from precursor II calcined at various temperatures are shown in Fig. 6. At 800 °C (Fig. 6a), coarse agglomerates and a large intergranular porosity are observed. The growth and densification of grains are not complete yet. At 1200 °C (Fig. 6b), large grains form islands in a sea of small grains. The grains are still mostly fragmented because of incomplete growth. At 1350 °C (Fig. 6c), a dramatic change in the microstructure is observed. The grain growth appears complete. A large-grained, uniform, pentagonal microstructure is observed with a 10 to 15 μm grain size. The powder microstructure of precursors I and III calcined at the same 1350 °C for 1 h are different from that of precursor II. For precursor I (Fig. 7a), a smaller-grained, irregular microstructure is observed with a grain size smaller than 5 μm. For precursor III (Fig. 7b), its microstructure is similar to that of precursor I except for having a larger intergranular porosity. The difference in grain size is also partially reflected in the measured dielectric constants. They are 2824, 825, and 2325 for BaTiO₃ prepared via precursors I, II, and III, respectively. The measured dielectric properties exhibit a strong dependence on grain size and diminish with increasing grain size. This observation accords with a report in the literature [18]. The measured Ba/Ti ratios, which could dramatically influence the microstructural de-

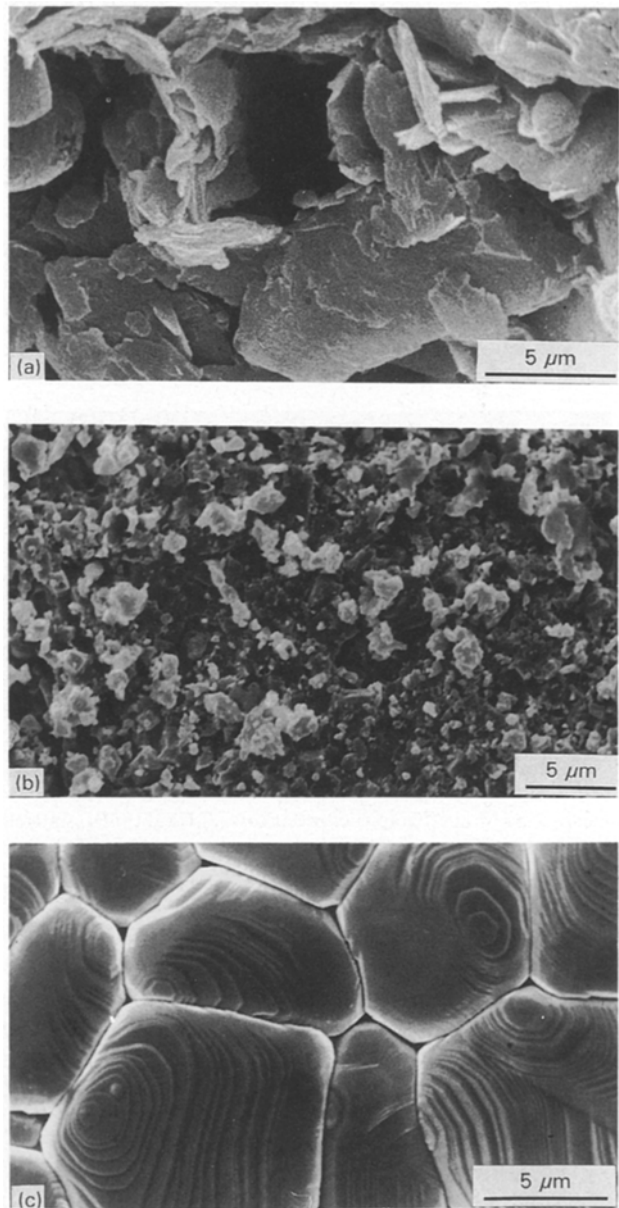


Figure 6 SEM micrographs of precursor II sintered under various conditions: (a) 1 h at 800 °C, (b) 1 h at 1200 °C, (c) 1 h at 1350 °C.

velopment in BaTiO₃ [9], have almost reached the theoretical value and range from 0.990 to 1.048. The results suggest that it is feasible to control the growth, size distribution, and microstructure of BaTiO₃ by using appropriate chelating agents.

4. Conclusion

The sol-gel preparation of BaTiO₃ from Ti(OR)₄ (R = isoC₃H₇ or C₄H₉) + Ba(CH₃COO)₂ + chelating agent CH₃COCH₂COR' (R' = CH₃ or OC₂H₅) yields an amorphous gel which crystallizes into a cubic phase after heating for 1 h at 650 °C and transforms into a tetragonal phase with *c/a* ratio of 1.0096 after heating for 1 h at 1350 °C. FT-IR and FAB-MS analyses suggest that the chelating agent substituted for one of the OR groups in Ti(OR)₄ to form Ti(OR)₃(CH₃COCHCOR'). The resultant increase in bonding and steric hindrance due to the dual carbonyl groups

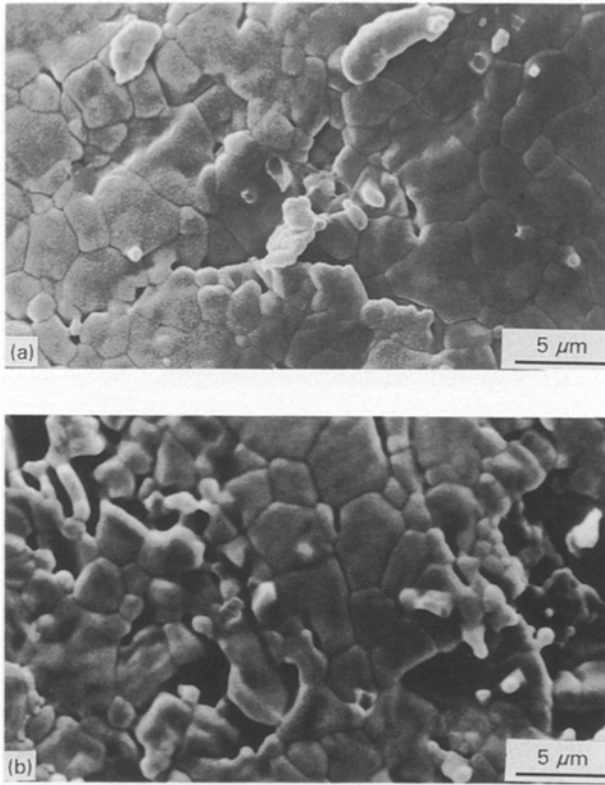


Figure 7 SEM micrographs of precursors (a) I and (b) III, sintered for 1 h at 1350°C.

in these chelating agents is responsible for the differences in gelation time and grain size. The gelation time varied from 3 to 5 months and diminished with increasing steric hindrance. The measured dielectric constants diminished with increasing grain size. The results illustrate the merits of altering the chemistry of the precursors to control the properties of the BaTiO₃.

Acknowledgements

Financial support by the National Science Council under Grant No. NSC-82-0208-M-007-101 is gratefully acknowledged.

References

1. U. SYAMAPRASAD, R. KGALGALI and B. C. MOHANTY, *J. Amer. Ceram. Soc.* **70** (1987) 147.
2. T. R. ARMSTRONG, K. A. YOUNG and R. C. BUCHANAN, *ibid.* **73** (1990) 700.
3. X. W. ZHANG, Y. H. HAN, M. LAI and D. M. SMITH, *ibid.* **70** (1987) 100.
4. H. L. HSIEH and T. F. FANG, *ibid.* **73** (1990) 1566.
5. G. KOSCHEK and E. KUBALEK, *ibid.* **68** (1985) 582.
6. K. KISS, J. MAGDER, M. S. VUKASOVICH and R. J. LOCKHART, *ibid.* **49** (1966) 291.
7. D. Y. WANG and UMEYA, *ibid.* **73** (1990) 669.
8. J. P. ZHONG, M. Y. ZHAO and H. WANG, *Ceram. Int.* **16** (1990) 85.
9. T. F. LIN and C. T. CHU, *J. Amer. Ceram. Soc.* **73** (1990) 531.
10. J. REHSRINGER and J. C. BERNIER, *Mater. Res. Soc. Symp. Proc.* **72** (1986) 67.
11. P. P. RHULE and S. H. RISBUD, *Adv. Ceram. Mater.* **3** (1988) 183.
12. J. LIVAGE, C. SANCHEZ, M. HENRY and S. DOEUFF, *Solid State Ionics* **32** (1989) 633.
13. A. YAMAMOTO and S. KAMBARA, *J. Amer. Chem. Soc.* **79** (1957) 4344.
14. S. J. MILNE and S. H. PYKE, *J. Amer. Ceram. Soc.* **74** (1991) 1407.
15. T. YOKO, K. KAMIYA and K. TANAKA, *J. Mater. Sci.* **25** (1990) 3922.
16. R. VIVEKANANDAN and T. R. KUTTY, *Powd. Technol.* **57** (1989) 181.
17. K. UCHION, E. SANDANAGA and T. HIROSE, *J. Amer. Ceram. Soc.* **72** (1989) 1555.
18. G. ARLT, F. HENNINGS and G. DE WIT, *J. Appl. Phys.* **58** (1985) 1619.

Received 8 November 1993
and accepted 22 April 1994